Detecting Buried Mines in Ground Penetrating Radar Using a Hough Transform Approach

Mark J. Carlotto (mark.carlotto@veridian.com)
Veridian Systems Division
P.O. Box 134008, 1975 Green Road, Ann Arbor, MI 48113-4008

Abstract

A method for detecting buried mines in ground penetrating radar (GPR) data using a Hough transform approach is described. GPR is one of three sensors used in the Mine Hunter/Killer (MH/K) system for detecting buried mines. A buried mine modeled as a point scatterer in object space gives rise to a hyperbolic response in GPR measurement space. Our approach uses the Hough transform to recover the object space representation (i.e., the location of mines in x, y, and depth) from the GPR data, in effect 'deconvolving' the response of the radar. This is done by having each point in measurement space vote for all points in object space where the mine could be located. Against a baseline energy detector, the Hough algorithm shows a one half order reduction in false alarm rate at a fixed probability of detection for low metal, metal, and non metal mines.

Introduction

Ground penetrating radar (GPR) is one of three sensors used in the Mine Hunter/Killer (MH/K) mine detection and neutralization system. The GPR used on the MH/K is a stepped frequency radar. Individually, each of the 20 antennas are excited with a sinusoidal tone. The tone is transmitted for a specified dwell time, then a sample of the earth response is taken. The sinusoidal tone is then stepped to the next frequency until 128 frequencies from 500 MHz to 2000 MHz have been transmitted and sampled. After the frequency scan the next antenna is scanned until all 20 have collected the 128 samples. After the vehicle moves 2”, the process repeats. The 128 frequency samples are processed into depth. This involves several steps including: calibration, ground surface rejection, and finally a 1D FFT in depth. Figure 1 shows the signature produced from a typical landmine. It is a 2D representation of the 3D data in which each panel shows 34” of along-track vs. depth return data. The panels correspond to adjacent antennas. The antennas are separated by 6”. For this example a hyperbolic signature may be seen in 4 of the 20 antennas. This roughly corresponds to a beamwidth of 85° in free space.

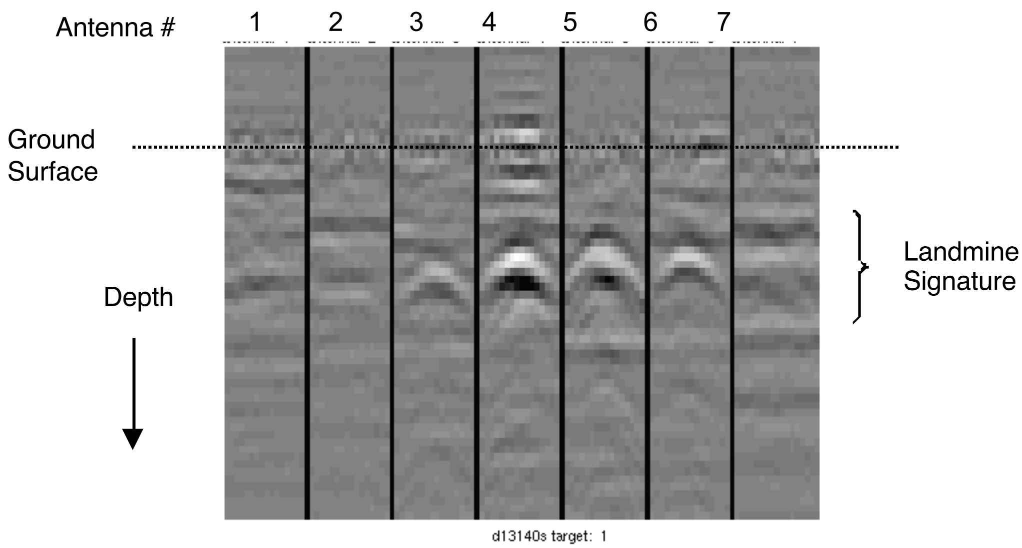

Figure 1 3-D signature of landmine depicted as series of 2-D data slices.

By exploiting the shape of the hyperbolic response, techniques such as the Radon transform and 3-D size/shape features are able to improve performance over detectors that respond only to the amount of energy reflected back from the mine (Marble et al 2001). In this paper a new algorithm based on the Hough transform is described, and preliminary results for MH/K data (Test 4) are presented and discussed.

Hough-Based GPR Mine Detection

The Hough transform is a method for finding geometric objects such as lines, parametric curves, and shapes in images (Hough 1962). For radar it has been used to detect features such as road intersections in SAR (Iisaka and Sakurai-Amano, 1996), low radar cross-section moving targets using multiple sensors (Cheng, Sun, Liu and Chen, 1997), and military formations in moving target indicator (MTI) data (Carlotto 2001).

Consider the problem of detecting linear arrangements within a set of points. The equation, $y = mx + b$ represents a line by its slope m and y-intercept b. In the Hough transform, each point votes for all lines (slope-intercept combinations) that can pass through it. Assume that a single linear arrangement of points is present. Since points that lie along a line vote for the same slope-intercept combination, as votes are added, those for the slope and intercept values of the line passing through the points exceeds those of other lines. In the Hough space of slope and intercept combinations, a peak forms at the location corresponding to the equation of the line in Cartesian space. Lines in Cartesian space thus map to points in Hough space, and vice versa.

With reference to Figure 2, a buried mine (modeled as a point scatterer) in object space (p, d) gives rise to a hyperbolic response in GPR measurement space (x, z). For a point scatterer at (p_0, d_0), the hyperbolic response is

$$z = \sqrt{\left(x - p_0\right)^2 + d_0^2} \tag{1}$$

for

$$\tan^{-1}\left(\frac{x - p_0}{z}\right) < \theta \tag{2}$$

where θ is the beamwidth of the radar.

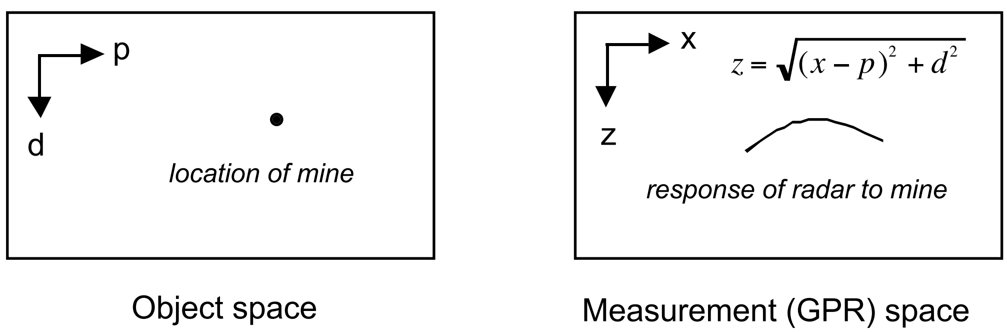

Figure 2 Object and GPR measurement spaces

Our approach here is to use the Hough transform to recover the object space representation from the GPR data, in effect 'deconvolving' the response of the radar. This is done by having each point in measurement space vote for all points in object space where the mine could be; i.e., for each x, z, and $d_i < z$

$$h(p, d) = \sum_{x,z} f(x, z) \sum_i \delta\left(p_i, d_i\right) \tag{3}$$

where the weight of a vote is equal to the magnitude of its GPR response $f(x, z)$, and

$$p_i = x \pm \sqrt{z^2 - d_i^2} \tag{4}$$

for $d_i < z$. In places where mines are located in object space, peaks form which can be detected using conventional CFAR techniques. Figure 3 is an example using simulated GPR data.

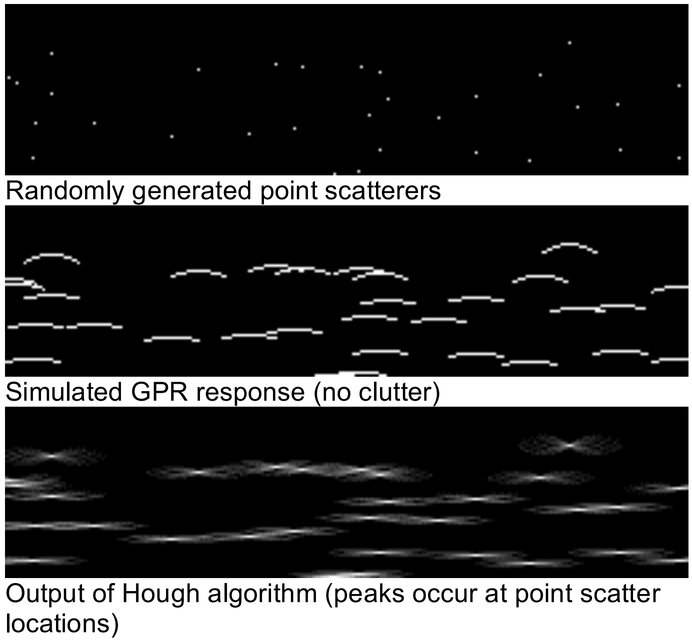

Figure 3 Example of Hough transform applied to simulated GPR data

Mine Detection Processing Architecture

Figure 4 shows the Hough transform algorithm embedded in an end-to-end GPR mine detection architecture. The dotted lines are alternative (bypass) paths that are used for comparing algorithm performance gains in the next section.

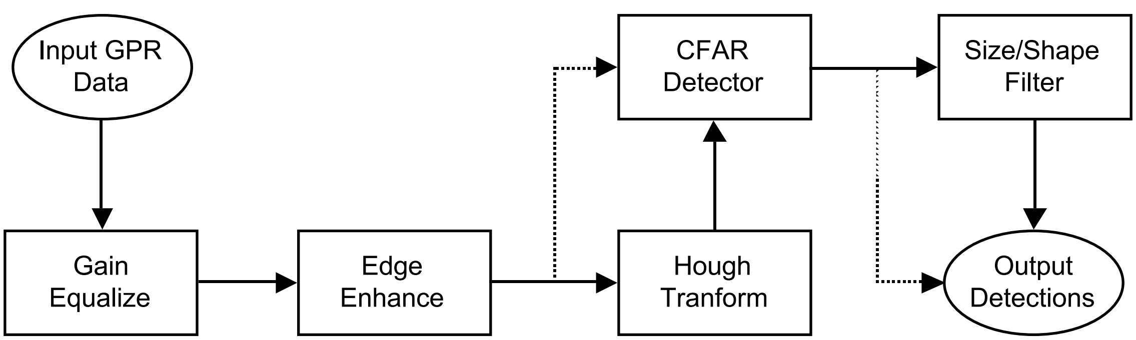

Figure 4 Mine detection processing architecture

The input is Sandia calibrated GPR data, $r_{n,m,k}$. In order to equalize gain differences we subtract the average response for each antenna at each depth over time and divide by the standard deviation of the response

$$g_{n,m,k} = \frac{r_{n,m,k} - \mu_{m,k}}{\sigma_{m,k}} \tag{5}$$

where n, m, and k index the antenna, the sample in time (i.e., as the vehicle moves over the terrain), and the depth, respectively, $\mu_{m,k} = \frac{1}{N}\sum_n r_{n,m,k}$ and $\sigma^2_{m,k} = \frac{1}{N}\sum_n \left(r_{n,m,k} - \mu_{m,k}\right)^2$.

The Hough transform algorithm functions like a family of matched filters, each designed to detect the hyperbolic response of a mine at a given depth. It is an optimal filter for detecting mines in the presence of additive white Gaussian (AWG) clutter. Subsurface soil and rock strata having different radar backscatter characteristics produce horizontal bands of clutter in GPR data. This clutter, which is not AWG, can obscure the return from a mine. Edge enhancement is performed in the along-track and cross-track directions to reduce the horizontal banding and to enhance changes in reflectance at each depth:

$$f_{n,m,k} = \left(g_{n,m,k} - g_{n-1,m,k}\right)^2 + \left(g_{n,m,k} - g_{n+1,m,k}\right)^2 + \left(g_{n,m,k} - g_{n,m-1,k}\right)^2 \tag{6}$$

Forward and backward differences are computed in the cross-track direction to provide data at the ends of the antenna array (n=0,N-1).

The Hough algorithm is applied to $f_{n,m,k}$ in the along track direction as described in Eqs. 3-4. This generates the 3-D volume $h_{n,m,k}$ which is collapsed into a 2-D image by summing over depth

$$i_{n,m} = \sum_k h_{n,m,k} \ . \tag{7}$$

To provide a baseline for measuring the processing gain of the Hough algorithm, a 'bypass' mode is provided to collapse the edge enhanced data $f_{n,m,k}$ into a 2-D image directly without Hough processing.

Summing over depth adds the edge enhancement/Hough responses staggered in 3-D space to form compact regions in a 2-D 'plan view' image of the data. The image is thresholded at a specified constant false alarm rate (CFAR), and the resultant detections processed as connected regions.

The following features are computed for each connected region: width, height, area, and the average energy over the region. Regions which do not satisfy the following user-specified size/shape requirements are eliminated:

$$\begin{aligned}
&(w_{\min} > \mathit{width} > w_{\max})\ \& \\
&(h_{\min} > \mathit{height} > h_{\max})\ \& \qquad (8)\\
&(f_{\min} > {}^{\mathit{area}}\!/_{\mathit{width} \times \mathit{height}} > f_{\max})
\end{aligned}$$

Remaining regions are rank-ordered by their energy and output as an ASCII file.

Figure 4 shows the output from the Hough algorithm collapsed into an image, the output of the CFAR detector, rank-ordered regions following size/shape filtering, and mine location ground truth data for comparison. The parameters used in this example and all experiments in Section 4 are given in Table 1.

Parameter	**Value**
CFAR	0.1
w_{min}, w_{max}	1, 7
h_{min}, h_{max}	5, 20
f_{min}, f_{max}	0.3, 1

Table 1 Processing parameter values used in all experiments

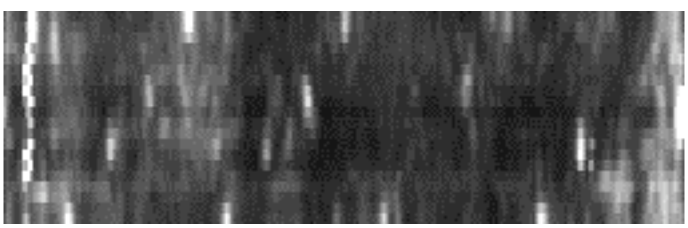
Output of Hough algorithm collapsed into 2D image


All detections, CFAR = 10%

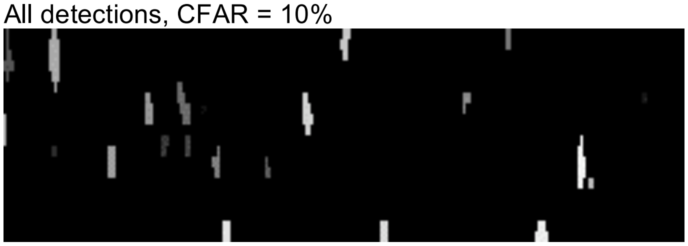
Ranked detections after size/shape filtering

Ground truth

Figure 5 Processing results from pass d11031s

Experimental Results

All passes in the Test 4 data set for runs 11-15 were processed with, and without the Hough transform, and with, and without size/shape filtering. ROC curves were computed for non-metal, low metal, and metal mines. Results are shown in Figures 6-9. For the area of each run processed, 1 false alarm is equivalent to 0.0067 FA/sq. meter

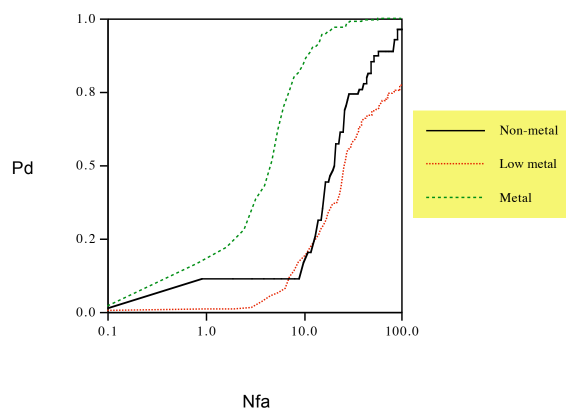

Figure 6 Results without the Hough transform and without size/shape filtering

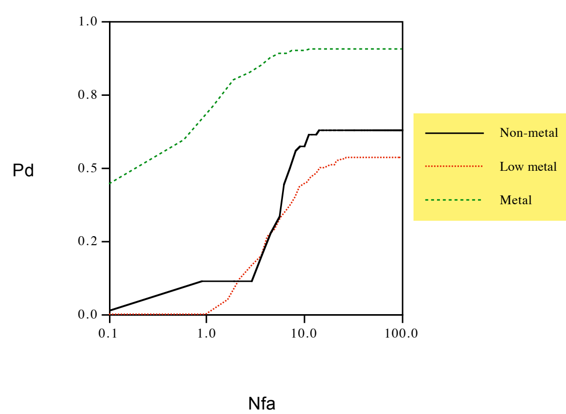

Figure 7 Results without the Hough transform and with size/shape filtering

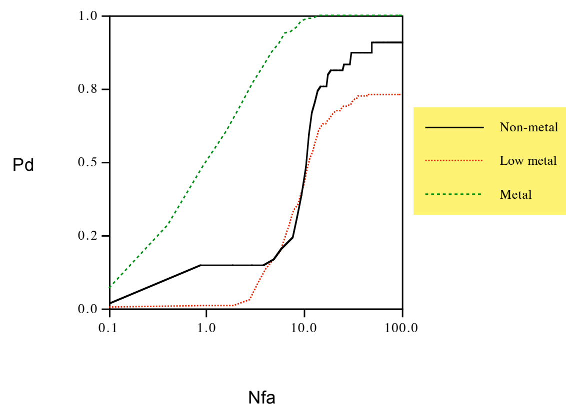

Figure 8 Results with the Hough transform and without size/shape filtering

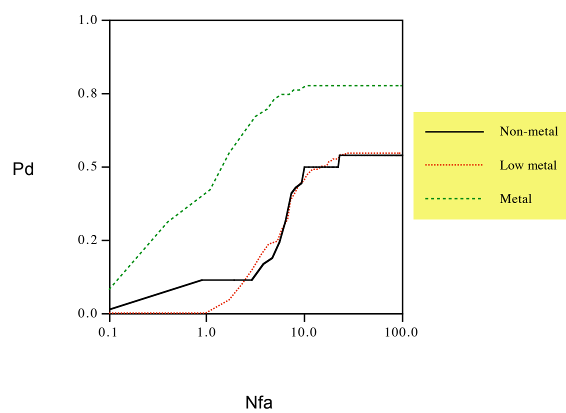

Figure 9 Results with the Hough transform and with size/shape filtering

To better visualize the comparative performance of the different detection approaches we plot the ROCs for all 4 processing options for each mine type in Figures 10-12. The options are:

Baseline	Without the Hough and without size/shape filtering
+SS	Without the Hough and with size/shape filtering
+H	With the Hough and without size/shape filtering
+H+SS	With the Hough and with size/shape filtering

These results show a definite processing gain in using the Hough algorithm (roughly one half order reduction in the FA rate at a given Pd). Size/shape filtering also reduces the FA rate but at the expense of a lower Pd. Results from processing with the Hough algorithm followed by size/shape filtering was no better than those without the Hough algorithm followed by size/shape filtering. This suggests that a different set of size/shape filtering parameters are needed for Hough processing, and that further improvements in performance may be achievable.

Conclusions and Future Work

A new algorithm for detecting mines in GPR data was developed and tested. The algorithm is based on detecting hyperbolic signatures of mines in the preprocessed Sandia data. One half order reduction in FA rates were achieved over all three mine types in the Test 4 data.

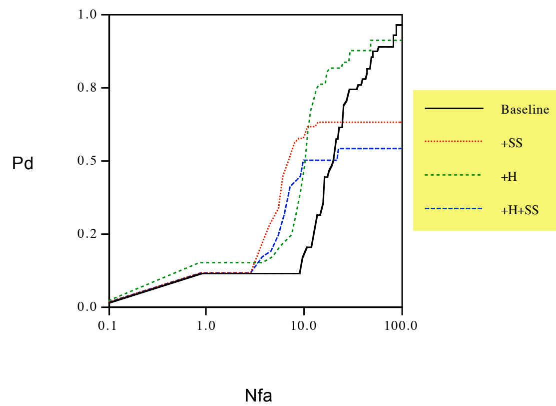

Figure 10 Results of all processing schemes for non-metal mines

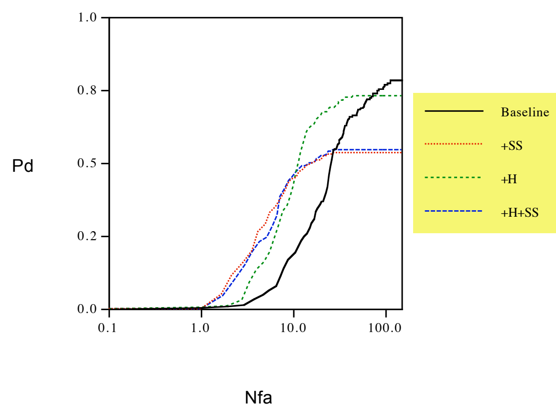

Figure 11 Results of all processing schemes for low metal mines

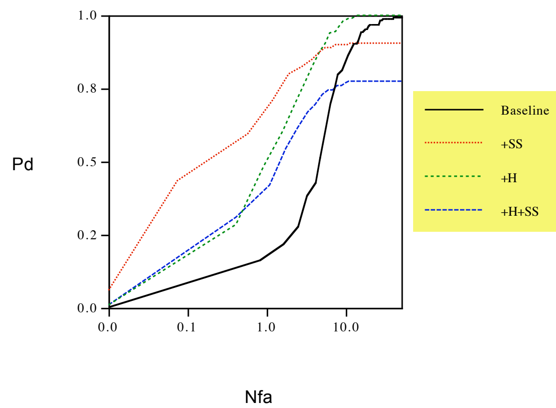

Figure 12 Results of all processing schemes for metal mines

In applying the Hough algorithm to the GPR data two problems were encountered. First, the precise shape of the radar returns were difficult to model. The Hough transform can be viewed as a matched filter whose impulse response varies with depth. It was difficult in practice to match the family of impulse responses to actual GPR data. Second, clutter returns frequently obscure the hyperbolic response of the radar to the mines. Three areas for future work are suggested: 1) Develop a means to better match the hyperbolic signatures modeled by the Hough transform to actual GPR signatures, 2) explore clutter reduction (e.g., whitening) techniques, and 3) perform additional testing and develop automated means for estimating optimal algorithm parameter values.

References

1. Jay Marble, Amber Iler, John Wegrzyn, and Mark Carlotto, "Buried Mine Detection Precessing for the Mine Hunter/Killer (MH/K) Vehicle," Veridian Systems, June 2001.
2. P.V.C. Hough, “Method and means for recognizing complex patterns,” US Patent 3,069,654, 1962.
3. J. Iisaka and T. Sakurai-Amano, "Automated GCP detection for SAR imagery: road intersections," *Proc. SPIE* Vol. 2818, 1996.
4. H. Cheng, Z. Sun, Q. Liu, and Y. Chen, "Small-target tracking technique with data fusion of distributed sensor net," *Proc. SPIE* Vol. 3163, pp. 566-574, 1997.
5. Mark J. Carlotto, "MTI Data Clustering and Formation Pattern Recognition," *IEEE Trans. Aerospace and Electronic Systems*, Vol. 37, No. 2, April 2001.